Rivista Italiana di Paleontologia e Stratigrafia
(*Research in Paleontology and Stratigraphy*)
vol. 124(1): 105-126. **March 2018**

# TAXONOMY AND EVOLUTIONARY RELATIONSHIPS WITHIN THE CALCAREOUS NANNOFOSSIL GENUS *ERICSONIA* IN THE UPPER PALEOCENE

ADELE GARZARELLA[1*] & ISABELLA RAFFI[1]

[1*]Corresponding author. Dipartimento di Ingegneria e Geologia, Università "G. d'Annunzio" di Chieti-Pescara, I-66013 Chieti Scalo, Italy.
E-mail: a.garzarella@unich.it

To cite this article: Garzarella A. & Raffi I. (2018) - Taxonomy and evolutionary relationships within the calcareous nannofossil genus *Ericsonia* in the upper Paleocene. *Riv. It. Paleontol. Strat.,* 124(1): 105-126.

*Keywords:* upper Paleocene; calcareous nannofossils; morphometry; *Ericsonia.*

*Abstract.* Detailed distribution ranges of the genus *Ericsonia* were obtained in the upper Paleocene interval from two deep-sea sections, ODP Site 1262 (South Eastern Atlantic Ocean) and Site 1215 (Eastern Equatorial Pacific Ocean), and were complemented with morphometric analyses with the purpose of clarifying the taxonomy of the Paleocene species ascribed to genus. The analysis on a high-resolution sampling set at ODP Site 1262 permitted to add information about the evolutionary relationship among the taxa included in the *Ericsonia* lineage, whose evolutionary emergence characterize the Paleocene nannofossil assemblages. Two taxonomic units have been validated in the Paleocene, *Ericsonia subpertusa* and *Ericsonia robusta* and they turned out to not have any evolutionary link. *E. robusta* shows substantial morphologic variability at cross-polarized light resulting in two endmember morphotypes, *E. robusta* morphotype A and *E. robusta* morphotype B. When observed at S.E.M., the two morphotypes have placoliths with a similar structure, therefore they document intra-specific variability. This is corroborated by the presence of specimens with intermediate morphologic features between the two endmembers, throughout the distribution range. *E. robusta* increases in abundance concomitantly with the sharp decline of *E. subpertusa* in mid Chron C25n. Subsequently, the highest occurrence of *E. robusta* morphotype B provides a distinct biohorizon coeval to the general decline of *E. robusta* within the upper Paleocene nannofossil assemblage.

## INTRODUCTION

The calcareous nannofossil genus *Ericsonia* represents a significant component of Paleogene assemblages. Since the first recorded occurrences in the stratigraphic record and its taxonomic description (Black 1964), the genus *Ericsonia* has been matter of taxonomic discussions on the various placoliths ascribed to it, characterized by highly variable morphology. Consequently, the species described and referred to *Ericsonia* by different authors (Bramlette & Sullivan 1961; Perch-Nielsen 1977, 1985; Wise & Wind 1977; Romein 1979; Okada & Thierstein 1979; Backman 1986; Bralower & Mutterlose 1995; Arny & Wise 2003; Raffi et al. 2005) reflected this taxonomic confusion. Some of these taxa, characterized by an elliptical outline, have been thereafter ascribed to the genera *Coccolithus* and *Reticulofenestra*, whereas other morphotypes, characterized by a circular outline, are still included in the genus and recognized as different species.

*Received: July 10, 2017; accepted: December 8, 2017*

According to the lineage of *Ericsonia* reconstructed by Romein (1979), three Paleocene species of circular *Ericsonia* can be distinguished and are evolutionally linked, *Ericsonia subpertusa*, *Ericsonia robusta* and *Ericsonia universa*. *Ericsonia robusta* developed from *E. subpertusa* in the late Paleocene (Thanetian) and was in turn ancestral of *E. universa*, that appeared just after *E. robusta* and was restricted to the same stratigraphic interval (Romein 1979; Fig. 35). Backman (1986) evidenced the biostratigraphic potential of *Ericsonia robusta* in a study of the upper Paleocene sediments of SW Atlantic (DSDP Site 528, Walvis Ridge). The biostratigraphic value of an *Ericsonia* species (referred to as *E. robusta* sensu Bramlette & Sullivan 1961; see taxonomic remarks below) was confirmed in a study of sediment cores from the paleo-equatorial Pacific Ocean (ODP Sites 1215A and 1221C; Raffi et al. 2005). This species provides a distinct highest occurrence biohorizon shortly above magnetochron C25n. Subsequently the results obtained in a biostratigraphic study of the continuous Paleocene succession of ODP Site 1262 (SW Atlantic area, Walvis Ridge; Agnini et al. 2007) evidenced two clear biohorizons correspon-

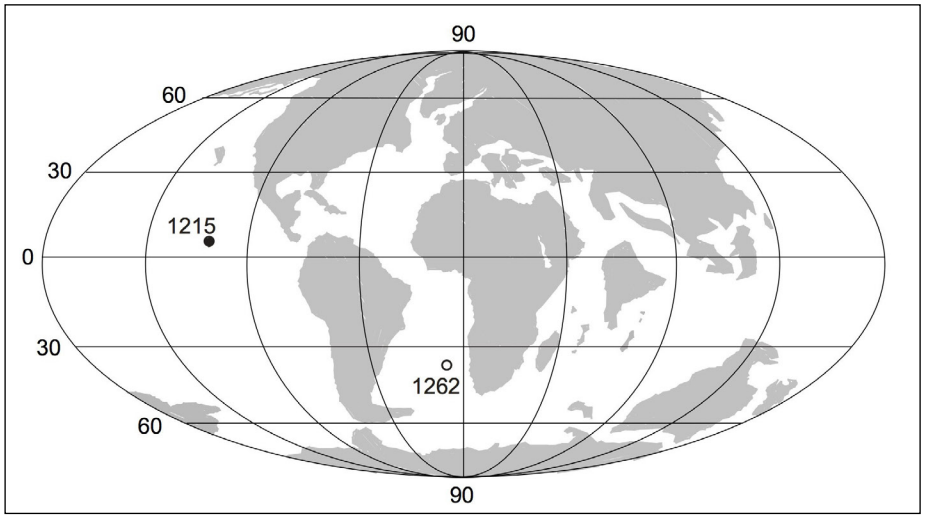


Fig. 1 - Paleogeographic map at 55 Ma with location of Sites 1262 and 1215.

ding to the lowest and highest occurrences of *E. robusta* in the interval corresponding to magnetochron C25n.

The availability of a higher resolution sample set from the same ODP Site 1262 succession studied by Agnini et alii (2007) prompted us to perform a detailed micropaleontological analysis on the genus *Ericsonia*, commonly present in the Paleocene. The aim is to possibly clarify the taxonomic issues related to the taxon delineating a simplified taxonomic approach for recognizing the Paleocene *Ericsonia* species at the polarizing microscope, and confirm or assert the reliability of the biostratigraphic signal provided by some species. Such a detailed analysis could help in reconstructing the upper Paleocene portion of *Ericsonia* lineage in a continuous section and documenting in detail the evolutionary relationships already inferred for the species (Romein 1979).

## Taxonomic remarks

As described above, the analyses of the rich and diversified assemblage of *Ericsonia* observed in upper Paleocene sediment cores from Pacific ODP Sites 1215 and 1221 and Atlantic ODP Site 1262 (Raffi et al. 2005; Agnini et al. 2007) (Fig. 1) evidenced a taxonomic unit labeled as *E. robusta* by those authors, and other *Ericsonia* specimens (*Ericsonia* spp. in Raffi et al. 2005). Some of these latter specimens were easily recognized as *Ericsonia subpertusa*, while others were difficult to be ascribed to defined species, due to the confused taxonomy resulted from different criteria and combinations proposed in the literature. Raffi et alii (2005) identified *Ericsonia robusta* mainly based on its large average size (> 9 μm up to 14 μm) and referring to the original description of Bramlette and Sullivan (1961) of *Cyclolithus? robustus*, as follows: "…Specimens large, circular, forming a thick ring, one side of which shows oblique striae… Open central area large and bordered by a narrow inner rim. Diameter 9–15 μ… Remarks: The large size and especially heavy or robust ring are distinctive features of the species but make the assignment to the genus/*Cyclolithus*/ questionable" (from Bramlette & Sullivan 1961). Raffi et al. (2005) included in their species concept specimens recognized as *Ericsonia* cf. *E. robusta* by Perch-Nielsen (1985; Figs 23-47, 23-48) and Bralower and Mutterlose (1995, plate 4, Figs. 9-12), and some of the specimens designated as *Heliolithus universus* by Wise and Wind (1977; plate 14, figs. 2-3) that were later referred as *E. universa* by Romein (1979).

Romein's *Ericsonia* species *Ericsonia robusta* and *E. universa* are distinguished using various criteria: the overall dimension; the ratio between the diameter of the central opening and the width of the margin of the placolith (ring or rim) (as summarized in Fig. 2); the extinction patterns observed at cross-polarized light, as the pattern of the sutures in distal or proximal view, and the angle between extinction lines and polarization directions. These extinction patterns reflect a complex arrangement of the elements in the placolith (see Romein 1979, pp. 108-110). Specifically, in the definition of *Ericsonia robusta,* Romein (1979) included specimens with a maximum diameter of 8-12 μm, and a ratio "*central opening diameter/ring width*" (opening D/ring

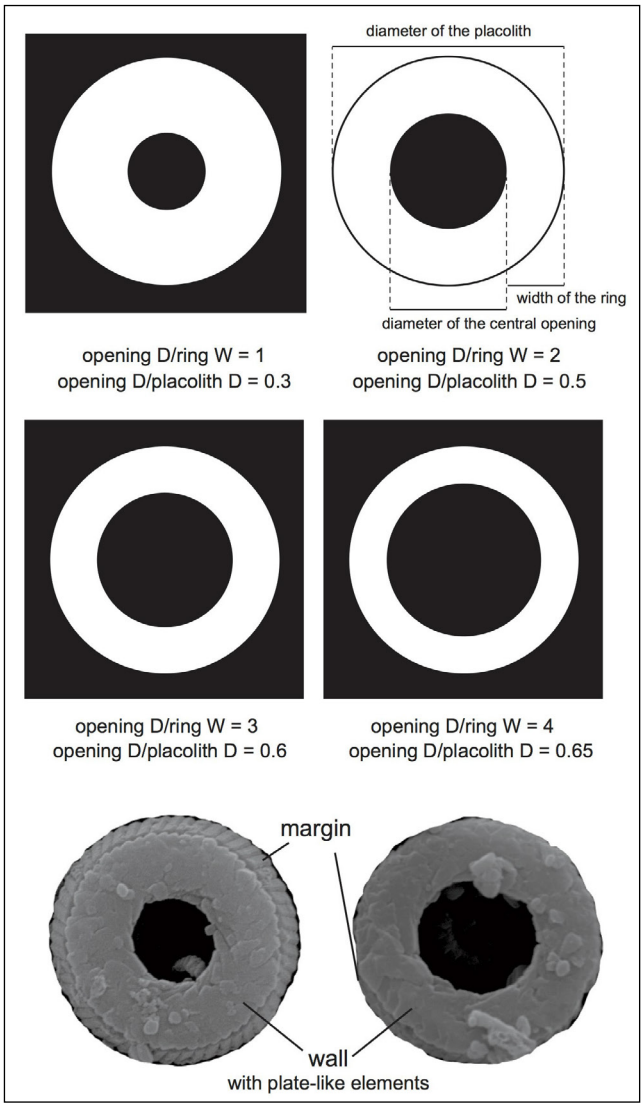


Fig. 2 - Measured morphometric parameters and schematic morphotypes of *Ericsonia*. For each morphotype the ratios "central opening diameter/ring width" (Romein 1979) and "central opening diameter/maximum placolith diameter" (opening D/placolith D; this study) are given.

W) ranging from 5 to 1, values that indicate highly variable area of the central opening and width of the margin. A similar complex arrangement of elements in distal and proximal shields of *Ericsonia robusta* is described for *E. universa* placolith (Romein 1979; p. 110; plate 10, fig. 14) that has a maximum diameter up to 16 μm, suggesting a generally larger size than *E. robusta*. For *Ericsonia universa* Romein (1979) did not give any reference value of the ratio "*central opening diameter/ring width*". Notably, the described complex arrangement of the cycles of the shields (composing the 'placolith') is rather difficult to be perceived with a polarizing microscope in both *Ericsonia* species. We include the *Ericsonia universa* specimens considered by Romein in our *E. robusta* taxonomic concept. Adding that intermediate forms between *Ericsonia robusta* and *E. universa* are commonly observed (Romein 1979; this study), hereafter we refer to as the *Ericsonia robusta* group.

A recent taxonomic revision within the genus *Ericsonia* by Bown (2016) proposed the establishment of several new species in the Paleocene interval, to somehow solve the taxonomic confusion related to the genus. The author studied Paleocene sediments from Tanzania (Kilwa Group), and described four new species (*Ericsonia aliquanta*, *E. media*, *E. monilis*, *E. orbis*) besides the known *E. robusta*, *E. staerkeri* and *E. subpertusa*. The taxa were differentiated on the basis of variable size of the placoliths and of the central area/opening, measured at the light microscope. Such a detailed differentiation was facilitated by the quality of nannofossil preservation the Tanzania sediments, representing a well known "Konservat Lagerstätte" for microfossils (Bown et al. 2008). The medium to large (> 5 μm) newly described species *Ericsonia media* and *Ericsonia aliquanta* were previously included in the definition of known species: *E. media* resembles to *E. subpertusa*, and *E. aliquanta* resembles to specimens of *E. robusta*.

In this study, we do not refer to the new species by Bown (2016) and prefer to maintain a conservative taxonomic concept for the Paleocene *Ericsonia* before performing our detailed morphometric analysis. This choice is justified by the general preservation of nannofossils in the Site 1262 sediments that show modest but persistent dissolution through the studied interval, often making difficult to differentiate small placoliths. The aim is to clarify the taxonomy of Paleocene *Ericsonia* and evaluate if potential new species, as those described by Bown (2016), are easly identifiable and, overall, how much biostratigraphically distinctive and meaningful are.

Summarizing, we delineated the distribution patterns (Fig. 3) of the following taxonomic units: I) *Ericsonia subpertusa*, that was unequivocally recognized at cross-polarized light, following the original description of Hay and Mohler (1967); II) *E. robusta* group, that corresponds to *E. robusta* - *E.universa* plexus and includes *Ericsonia* specimens with variable maximum size (6 to 15 μm) and central opening size, occasionally showing intermediate morphologic features between the end-members *E. robusta* and *E. universa* sensu Romein (1979).

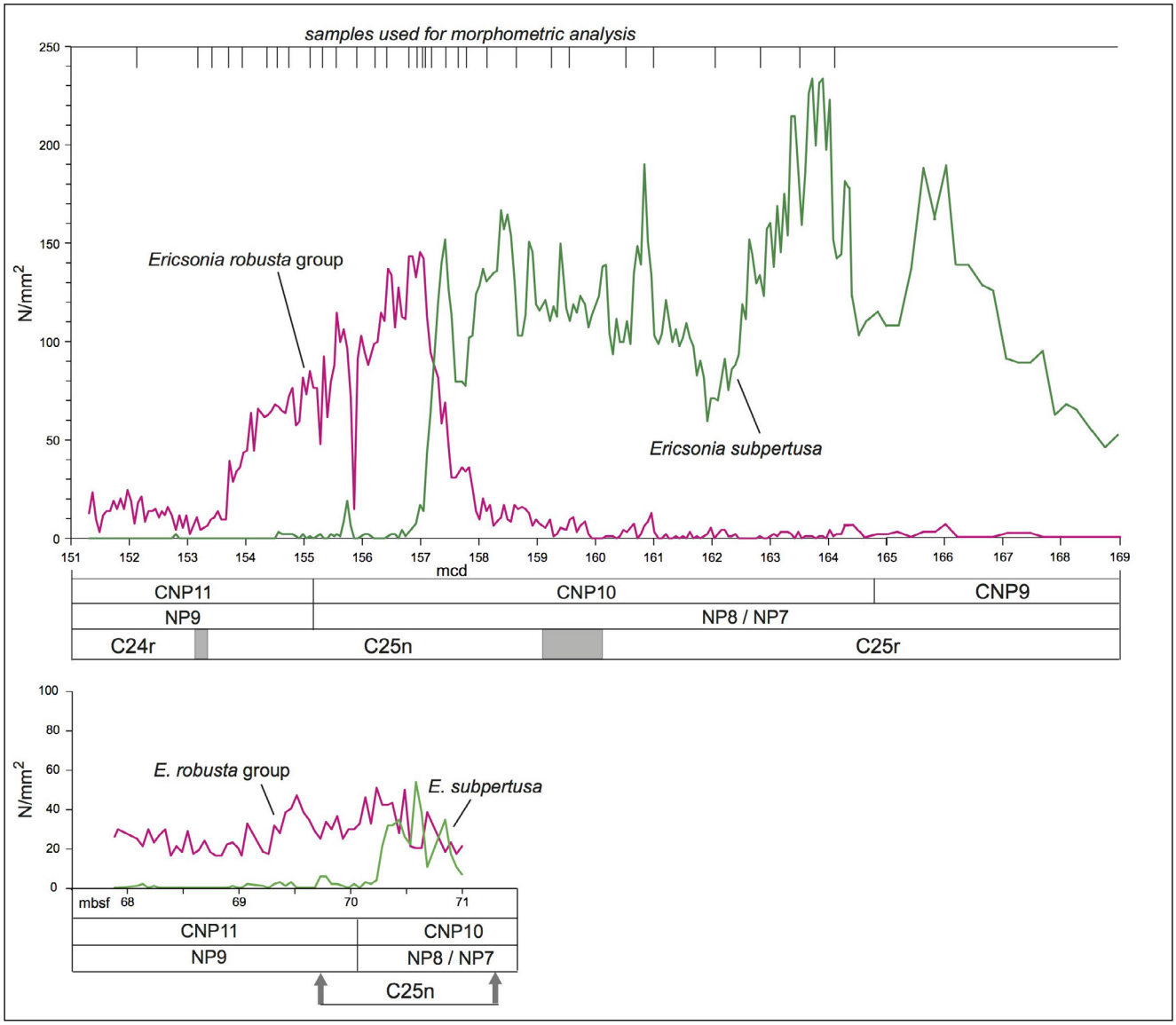


Fig. 3 - Distribution ranges of *Ericsonia subpertusa* and *Ericsonia robusta* group at ODP Sites 1262 and 1215, with biostratigraphy (Agnini et al. 2007; this study; Raffi et al. 2005) and paleomagnetic stratigraphy (Bowles 2006). Position of the selected samples from Site 1262, used for morphometric analysis, is reported. *mcd*: meter composite depth; *mbsf*: meter below sea floor.

## Material and methods

We evaluated quantitative abundance distribution of the considered taxonomic units throughout the upper Paleocene interval at Atlantic ODP Site 1262 and Pacific ODP Site 1215 (Fig. 1). Subsequently, a morphometric analysis on the observed *Ericsonia* morphotypes was carried out in selected samples from Site 1262.

### Location of sites and sampling

ODP Site 1262 was drilled as part of the Leg 208 Walvis Ridge depth transect (Zachos et al. 2004), located in the eastern South Atlantic (Lat. 27° S). It is the deepest site (water depth of 4759 m) and was placed at a paleolatitude of ~34°S and paleodepth of ~3600 m in the early Paleogene (Zachos et al. 2004) (Fig. 1). The Site 1262 sedimentary succession mainly consists of nannofossil oozes, with variable portions of clay, and is complete and undisturbed through Paleocene to middle Eocene. The 236 samples analyzed are part of the sample set used for previous high resolution stable isotope studies (Zachos et al. 2010; Littler et al. 2014). They are placed at an average spacing of 5-6 cm in the uppermost Paleocene section, from ~151 mcd to ~164 mcd, and 18-20 cm in the lowermost ~5 meters of the succession.

ODP Site 1215 was drilled in the central equatorial Pacific Ocean (Lat. 26°N) as part of Leg 199

"The Paleogene Equatorial Transect" and located at a paleolatitude of ~4°N in the early Paleogene (Lyle et al. 2002) (Fig. 1). Its sedimentary succession consists of upper Paleocene-lower Eocene nannofossil ooze or chalk with cherts, resting upon a basalt basement. Following a previous low-resolution analysis of the upper Paleocene core section at Site 1215A (Raffi et al. 2005), we increased the sampling resolution to 5 cm spacing and processed and studied 57 samples from the interval between ~68 to ~71 mcd.

All the samples from Sites 1262 and 1215 were processed to obtain smear slides following the technique of Bown & Young (1998).

### Chronology and biostratigraphy

The studied interval extends from the oldest magnetochron C25r to the youngest magnetochron C24r, and correlates with nannofossil Zones CNP 9 to lowermost CNP11 of Agnini et al. (2014) (= Zones NP7 to base NP9 of Martini 1971). According to the available chronology for Site 1262 (Westerhold et al. 2008; Littler et al. 2014) the time interval is included between ~57.6 and ~56.5 Ma. The core section studied at Site 1215 partially overlaps the interval studied at Site 1262, and corresponds to a time interval between ~57.5 Ma and ~56.5 Ma, encompassing most of Chron C25n and the lower part of Chron C24r. This approximate chronology for Site 1215 sediments has been obtained through linear interpolation between C25r/C25n and C25n/C24r reversal boundaries, as recognized at Hole 1215A (Lyle et al. 2002; Bowles 2006).

The temporal resolution of the sampling at Site 1262 and Site 1215 is ~5.0 kyr and ~15.0 kyr, respectively.

### Analyses on *Ericsonia* specimens

Analysis of the smear slides was carried out using light-microscope techniques under transmitted and cross-polarized light, at X1200 magnification. Abundance patterns of *Ericsonia subpertusa* and *E. robusta* group (Fig. 3) were obtained by counting the number of specimens in a prefixed area (N/mm$^2$ obtained from number of specimens in 30 field of view).

In the analysis of *Ericsonia* specimens, besides the diameter of the placolith and the central area, we considered the extinction and colour patterns observed in cross-polarized light. We observed the

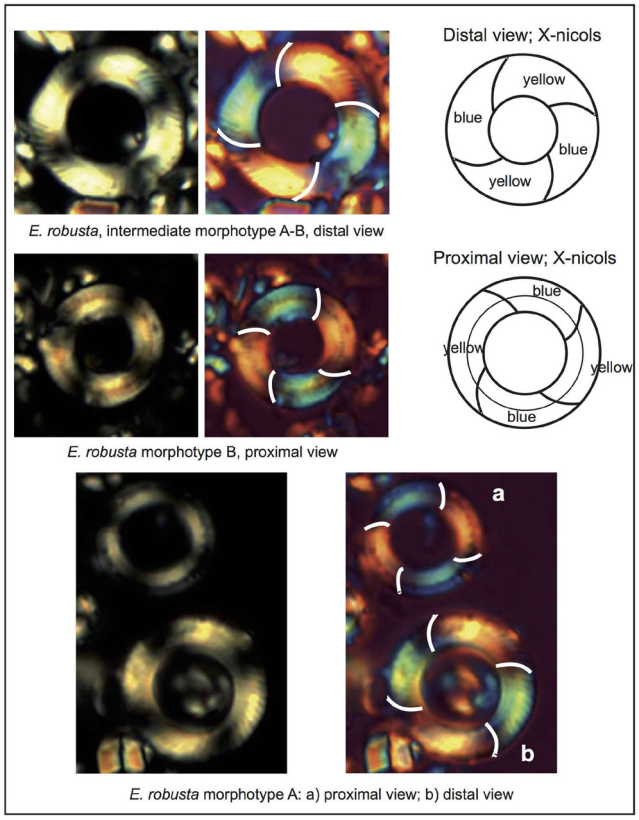


Fig. 4 - The use of the gypsum plate in cross-polarized light for distinguishing distal and proximal view of *Ericsonia* placoliths, based on different color (blue-yellow) distribution in the four sectors between extinction lines.

shape and sharpness of the extinction cross, the brightness of the simple or composite cycle of elements assembled to form the placolith, and the colour pattern with a gypsum plate inserted in the light-beam in cross-polarized light. The patterns are useful to recognize the proximal or distal sides in each observed placolith, following the method suggested by Romein (1979). The method permits to distinguish which side of the observed specimen is lying upward, since the structures of calcite crystal arrangement in the proximal side are different from the distal sides. The two sides were distinguished observing the direction (clockwise or counterclockwise) of the extinction lines and the different colours of sectors between them (Fig. 4). The four sectors appear alternately blue and yellow: the sectors blue in distal view become yellow in proximal view, and vice versa.

Morphometric analyses of the *Ericsonia* specimens were performed using image analyses software "Image-pro plus 7.0" in 30 samples from ODP Site 1262, selected at specific levels throughout the distribution range (Fig. 3). The number

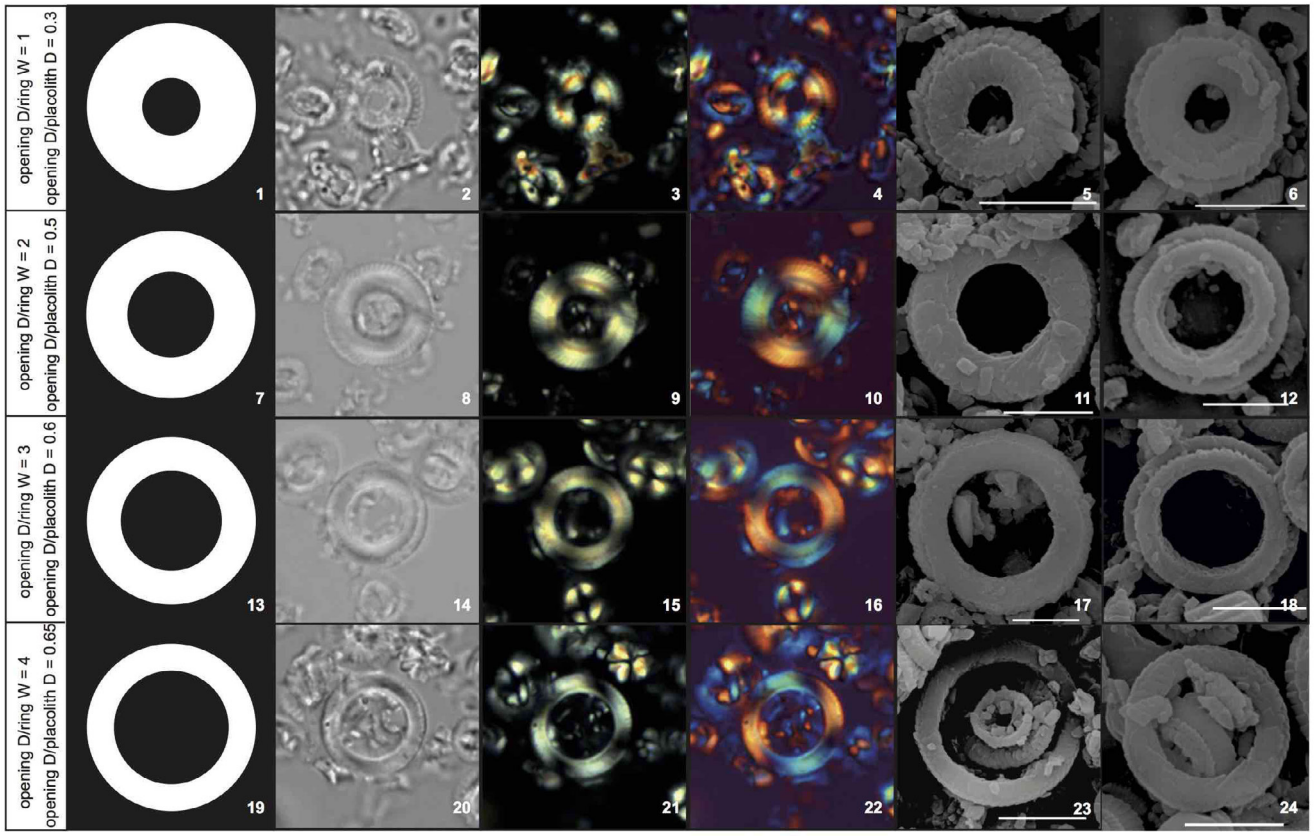


Fig. 5 - Schematic morphotypes of *Ericsonia* and corresponding photomicrographs at L.M., normal, cross-polarized light, with gypsum plate inserted, and at S.E.M.

of measured specimens varied accordingly with the abundance of the observed *Ericsonia* taxonomic units in the considered sample, generally from 35 to 50 specimens. In samples with high morphological variability within *Ericsonia* population, 80 to 100 specimens were measured. The diameter of the central opening (*opening D*) relative to the maximum diameter of the placolith (*placolith D*) was considered a useful parameter for characterization of the different morphotypes (Fig. 2), and calculated the ratio "*opening D/placolith D*". Practically, we followed the suggestion of Bralower and Muttelose (1985; p. 57) who "used an arbitrary limit of relative diameter of the central opening to distinguish" *E. subpertusa* from *Ericsonia formosa*. Relation between our ratio "*opening D/placolith D*" to the ratio values (i.e. opening D/ring W) suggested by Romein (1979) is reported in Fig. 2. The biometric data were processed using the PAST software (Hammer et al. 2001).

Subsequently, observation at the Scanning Electron Microscope (SEM) was used for comparing the structures of the placolith in the different taxonomic units considered.

## Results

During the counting of *Ericsonia robusta* gr. specimens under polarized light microscope, we observed a morphotype characterized by a large central opening (> 3 μm) relative to the maximum diameter (ranging from 7 to 11 μm), and by an extinction pattern in cross-polarized light that appears as a thick ring with a bright inner margin (Fig. 5, 13- 24; Pl. 1, figs 4-10; 23-25; 33-35; 39-40). Based on these features, it could be included in the morphological variability of *E. robusta* sensu Romein (1979). However, we considered it as a separate "morphotype" from the specimens matching the *Ericsonia robusta* sensu Raffi et al. (2005) that appear brighter in cross-polarized light and has a relative smaller central opening (Fig. 5, 7-12; Pl. 1, figs. 21-22; 26-32; 36-38). Therefore, we distinguished two morphotypes within the *Ericsonia robusta* gr., *E. robusta* morphotype A and *E. robusta* morphotype B, the latter corresponding to *E. robusta* sensu Raffi et al. (2005). Thinking them as possibly being indicative of two different species (e.g. the smaller specimens

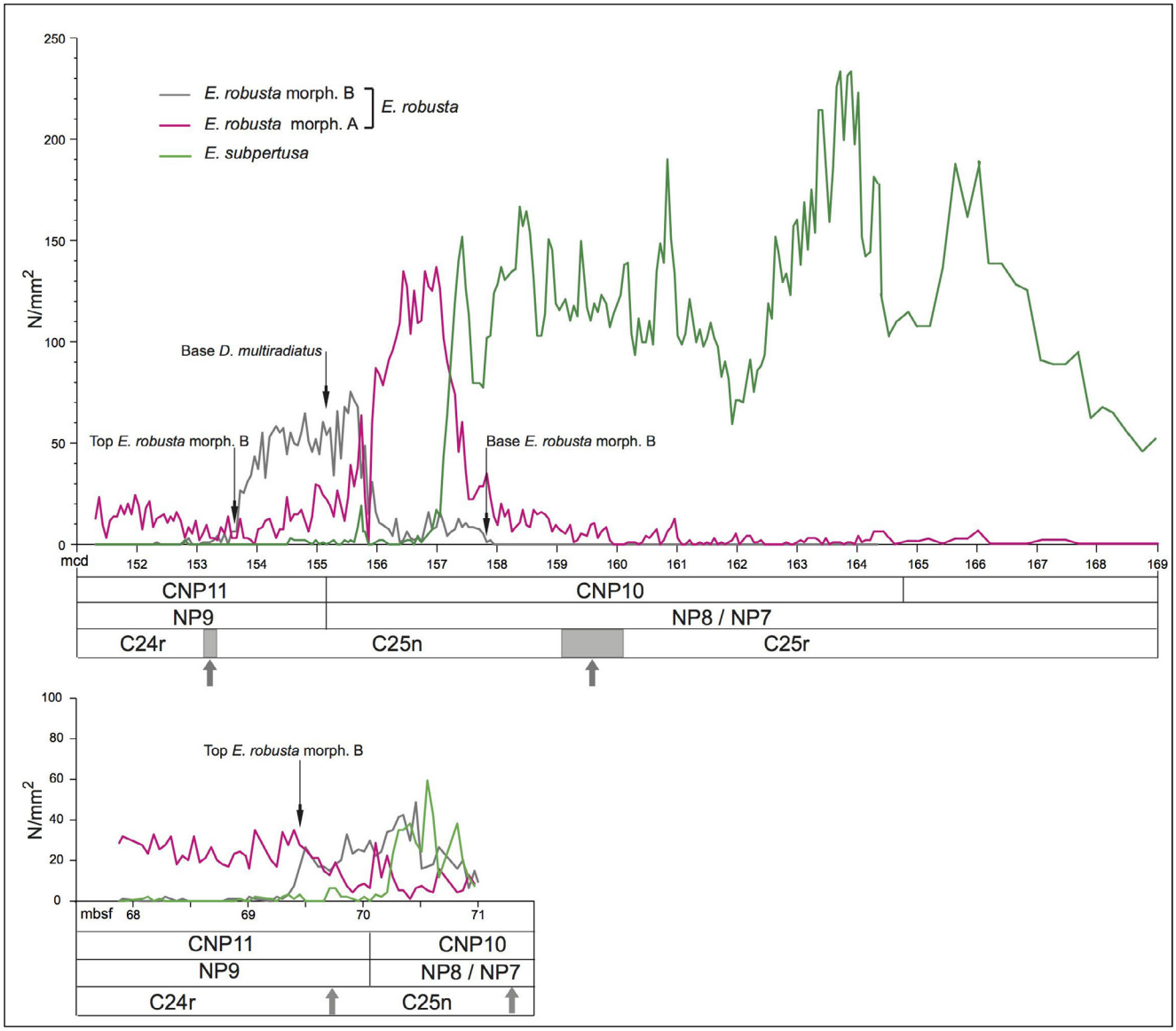


Fig. 6 - Distribution ranges of *Ericsonia subpertusa* and *Ericsonia robusta* morphotypes A and B at ODP Sites 1262 and 1215, with biostratigraphy (Agnini et al. 2007; this study; Raffi et al. 2005) and paleomagnetic stratigraphy (Bowles 2006).

of morphotype A resemble to *E. aliquanta* of Bown, 2016), we examined in detail their distribution and abundance patterns and the results from morphometric analysis with the aim to clarify further their taxonomy.

**Abundance patterns**

The abundance patterns of the considered taxonomic units of Paleocene *Ericsonia* at Sites 1262 and 1215 are showed again in Fig. 6, in which the distributions of *E. robusta* morphotypes A and B are separately reported. The data obtained at ODP Sites 1262 section are more complete because the studied interval encompasses the whole magnetochron C25n, and permitted to depict in detail the evolutionary development of the genus.

As expected, a gradual increase in variability of morphology and size within the *Ericsonia* assemblage is observed through the studied interval. In the lower part of Site 1262 section (from 164.34 to ~157 mcd, at ~57.6 to ~57 Ma) *Ericsonia subpertusa* prevails in the assemblage, reaching higher values (up to 233.5/mm$^2$) around 164 mcd, and only rare specimens of *E. robusta* morphotype A are present (Fig. 6). In the interval above starting from ~158 mcd, morphotype A has a distinct stratigraphic distribution and shows a rapid increase in abundance concomitantly with the occurrence of *E. robusta* morphotype B, thus delineating a sharp turnover in abundance with *E. subpertusa* (at ~157.2 mcd).

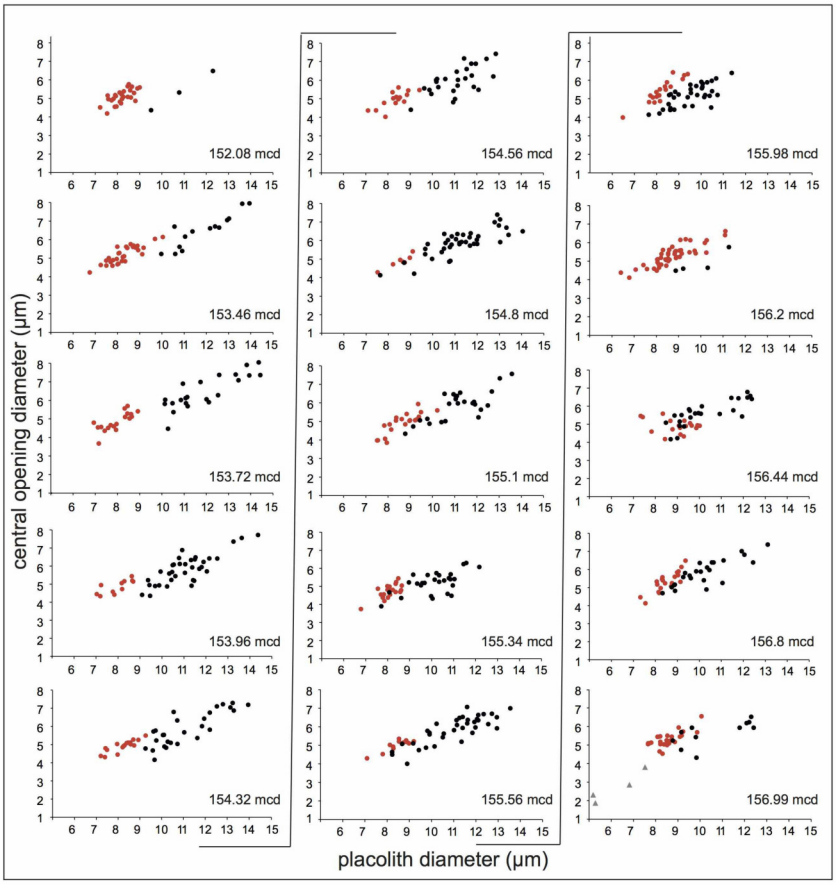


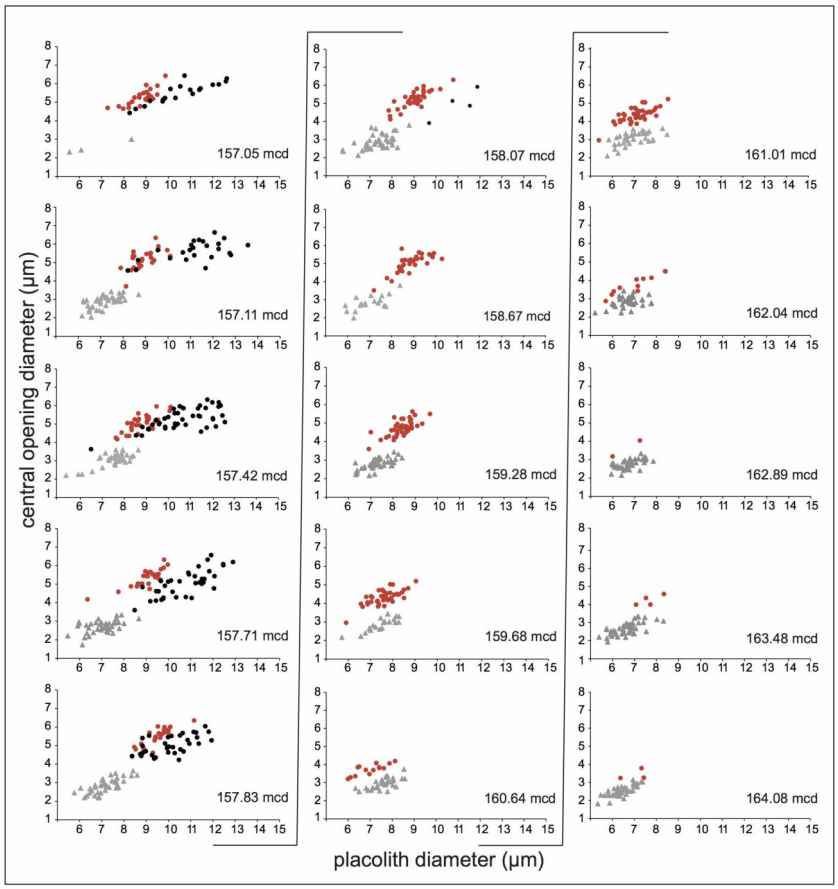


Figs 7 a-b - Results of morphometric measurements of *E. subpertusa* (grey triangle), *E. robusta* morphotype A (red dot) and *E. robusta* morphotype B (black dot) in the 30 selected samples. The maximum diameter (*placolith D*) is plotted vs. the diameter of the central opening (*opening D*) for each measured specimen.

Within a 1.2 m-interval of core sediments (between ~157.2 and 156 mcd) corresponding to ~0.1 m.y. time-interval, morphotype A significantly outnumber both the morphotype B and *E. subpertusa*. Few specimens of *Ericsonia* are difficult to be ascribed to *E. robusta* morphotypes A or B because they have intermediate morphologic features between the two, namely a size similar to morphotypes B but a lighter birefringence (Pl. 1, figs. 11-20; Pl. 2, figs. A and D). These specimens mostly occur in an interval straddling the Base of *E. robusta* morphotype B.

In the upper part of Site 1262 section (from ~156 mcd upward), the abundance of *Ericsonia robusta* morphotype A gradually drops in coincidence with the interval of high abundance of *E. robusta* morphotype B and with the final decline of *E. subpertusa*. The highest occurrence (Top) of morphotype B provides a prominent biostratigraphic signal at 153.38 mcd (corresponding to ~56.6 Ma) that is close to (just below) the top of Chron C25n (153.31-153.18 mcd). This biohorizon is placed in a similar stratigraphic position of Agnini et alii (2007), above Base of *Discoaster multiradiatus* (at 155.3 mcd, ~56.8 Ma), but it is more precisely defined here. *Ericsonia robusta* morphotype A is continuously

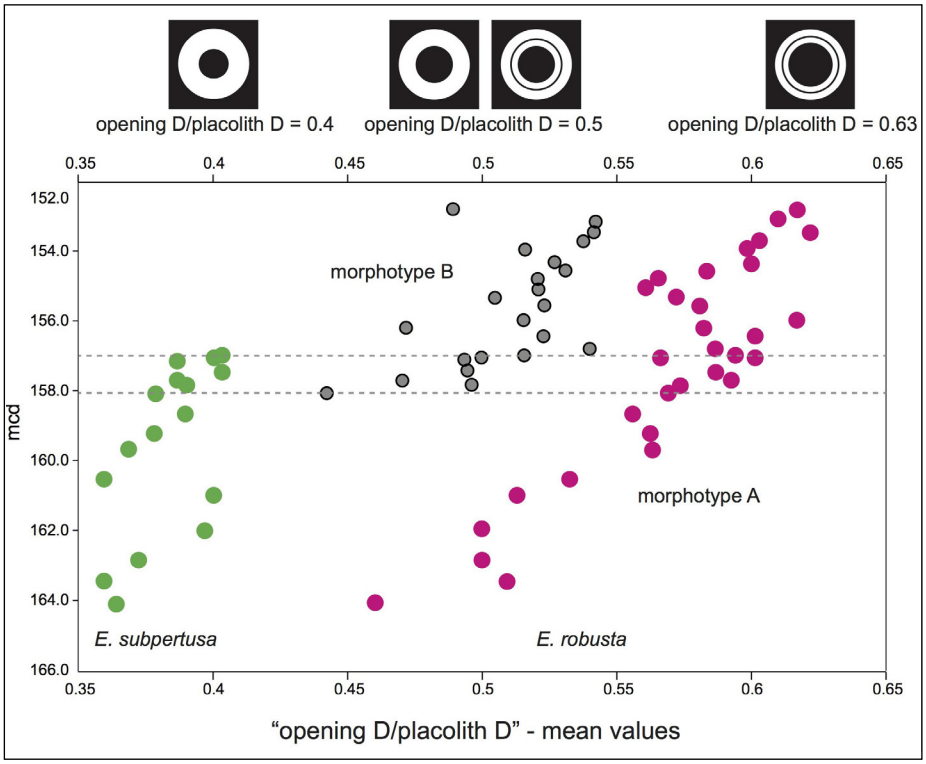


Fig. 8 - The mean values of the ratio "*opening D/placolith D*" in each sample used for morphometry through the studied section.

present in low abundance up to the top of the studied section at Site 1262.

The abundance patterns of *Ericsonia* taxonomic units at Site 1215 have been obtained in a shorter stratigraphic interval than the interval at ODP Site 1262, encompassing only part of Chron C25n and the lower part Chron C24r (between 71 and ~68 mcd). In this section, the patterns appear different: the three considered taxa show different proportions, *Ericsonia robusta* morphotype A never exceeds in abundance *E. robusta* morphotype B, although in the upper part of the range its abundance is generally higher (average of 30-40 specimens/mm$^2$) than the abundance observed in the coeval interval at Site 1262 (average of 20-30 specimens/mm$^2$). These differences observed in the *Ericsonia* assemblages of the two sites could be partly explained as due to preservation problems, because the nannofossil assemblage in the sediments of Site 1215 are affected by pervasive dissolution that favoured robust placoliths like *Ericsonia* that increased their relative abundance.

Tab. 1 -Statistics of measured parameters of genus *Ericsonia* in the studied section at Leg 208 ODP Site 1262.

| | | oD/pD | Placolith diameter (µm) | Opening diameter (µm) |
|---|---|---|---|---|
| *E. subpertusa* | Min | 0,3 | 5,4 | 1,7 |
| | Max | 0,5 | 9 | 4 |
| | Mean | 0,38 | 7,23 | 2,77 |
| | Stand. dev | 0,05 | 0,64 | 2,77 |
| | Median | 0,4 | 7,3 | 2,8 |
| | Number of measurements | 560 | 560 | 560 |
| *E. robusta* A | Min | 0,4 | 5,9 | 2,8 |
| | Max | 0,7 | 11,6 | 6,7 |
| | Mean | 0,60 | 8,55 | 4,95 |
| | Stand. dev | 0,05 | 0,85 | 0,64 |
| | Median | 0,6 | 8,6 | 5 |
| | Number of measurements | 701 | 701 | 701 |
| *E. robusta* B | Min | 0,4 | 6,6 | 3,6 |
| | Max | 0,6 | 14,5 | 8 |
| | Mean | 0,51 | 10,85 | 5,56 |
| | Stand. dev | 0,06 | 1,31 | 0,79 |
| | Median | 0,5 | 10,8 | 5,5 |

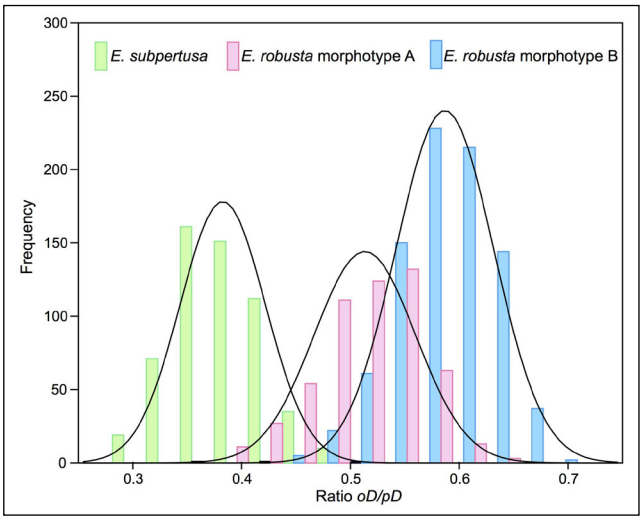


Fig. 9 - Results of mixture analysis applied to the ratio "*opening D/placolith D*" measured in the *Ericsonia* pool.

## Morphometric analysis

The results of morphometric measurements of the three taxonomic units considered are reported in Figure 7 a-b that shows bivariate plots of the maximum diameter (*placolith D*) vs. the diameter of the central opening (*opening D*) of the measured placoliths in the 30 selected samples. The measured parameters and their minimum and maximum values are reported in Table 1, together with the mean values of the ratio "*opening D/placolith D*" (labelled "*oD/pD*" hereafter) of each taxonomic unit. The plot of the mean values of *oD/pD* of the *Ericsonia* morphotypes through the section (measured in each sample used for morphometry) shows a general increase up-section (Fig. 8). This increase is subtle in *Ericsonia subpertusa*, whereas it is noticeable in *E. robusta*, overall in morphotype A. In the interval with the concomitant occurrence of *Ericsonia subpertusa* and *E. robusta* morphotypes A and B (grey area in Fig. 8) the respective mean *oD/pD* values are remarkably distinct.

Results of mixture analysis of all the *oD/pD* values are show in Fig. 9, and permitted to identify which kind of frequency distribution is displayed. Distribution of the ratio values in each considered sample is showed in the histograms of Fig. 10 and Fig. 11, with Gaussian Kernel density plots included. This smooth density estimator of histograms provides an overview on the distribution of measured parameter, in this case the ratio oD/pD. Kernel density is a non-parametric estimation of the probability density function of a random variable, and provides more accurate results than those observed in histograms. The advantage of using the Kernel density plots is that they permit to obtain a better overview of the frequency distribution of the ratio oD/pD in sample-specific histograms (Fig. 10 and Fig. 11).

In some samples from the lower part of the studied interval (Fig. 7a), the first specimens of *Ericsonia robusta* morphotype A are very rare and are similar in size to the dominant *E. subpertusa*. The

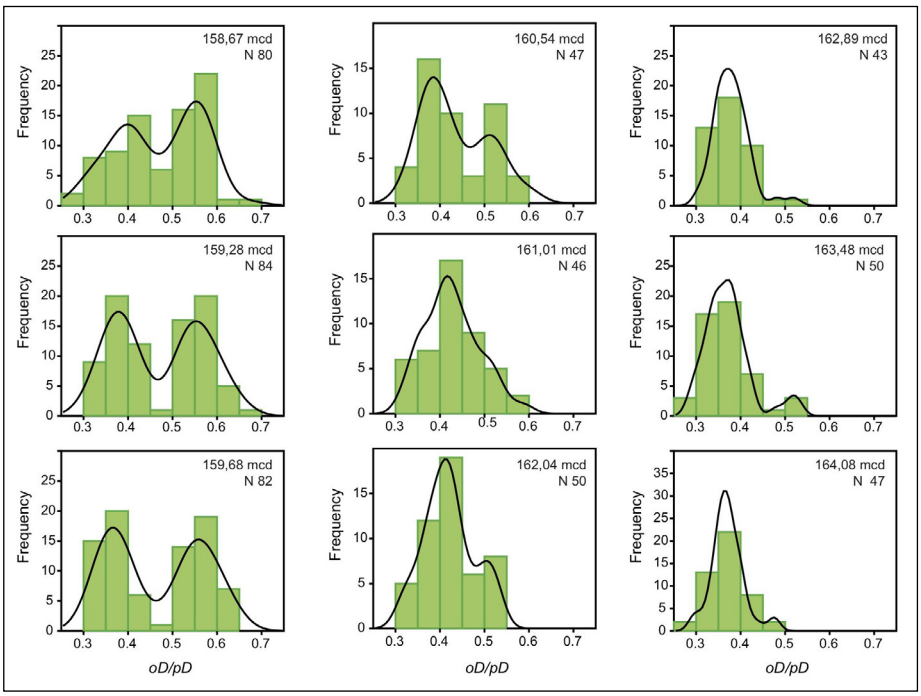


Fig. 10 - Single sample histograms and Gaussian Kernel density plots applied to the ratio "*opening D/placolith D*", measured in specimens of *Ericsonia subpertusa* and *Ericsonia robusta* morphotype A in the lower part of the studied ODP 1262 section. Bins are 0.05-large in each sample. Gaussian Kernel density plots are included.

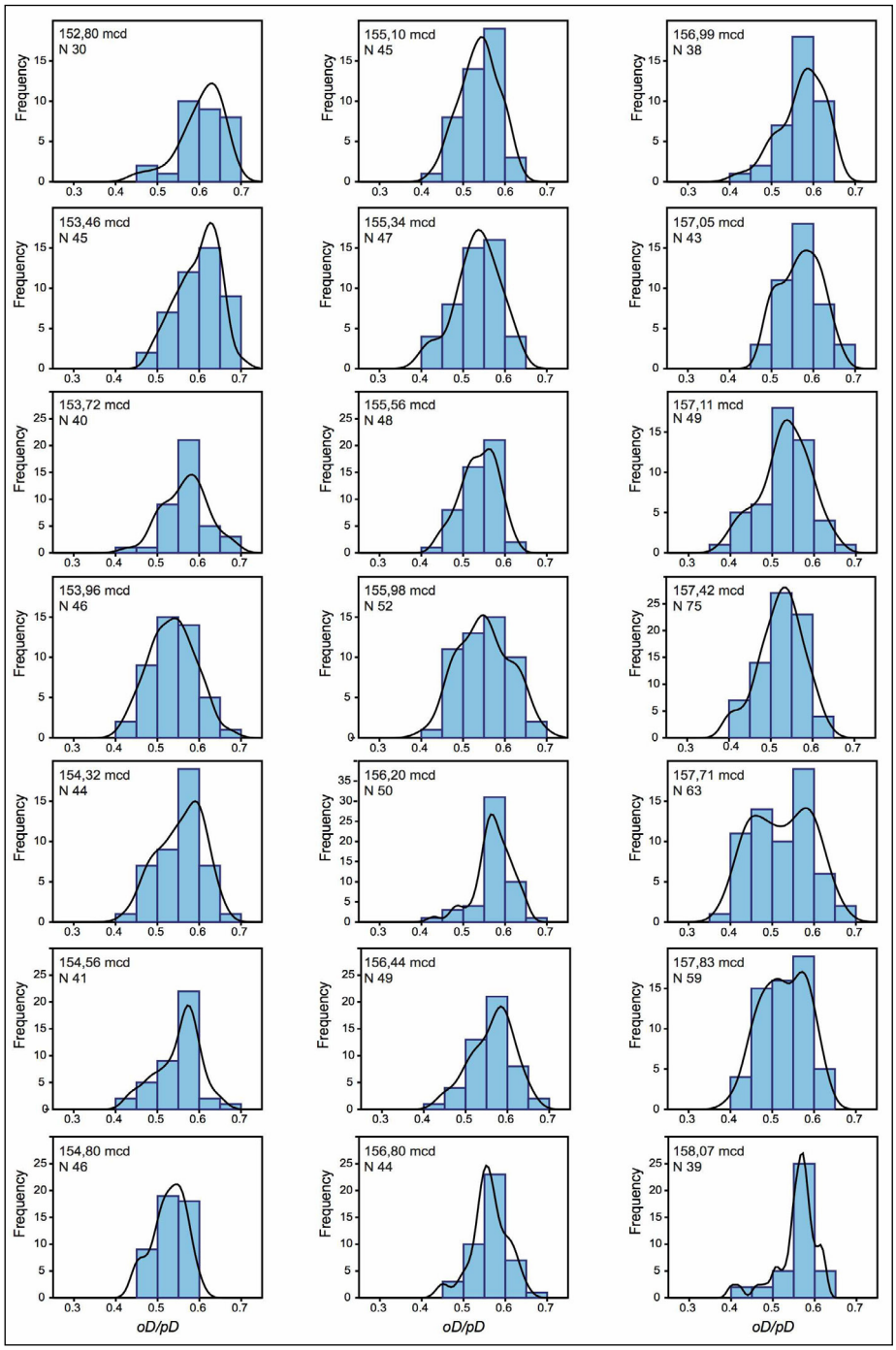


Fig. 11 - Single sample histograms and Gaussian Kernel density plots applied to the ratio "*opening D/placolith D*", measured in specimens of *Ericsonia robusta* morphotype A and morphotype B in the upper part of the studied ODP 1262 section. Bins are 0.05-large in each sample. Gaussian Kernel density plots are included.

distinction between the two taxa becomes evident from 160 mcd upwards, where *Ericsonia robusta* morphotype A increases in abundance. Accordingly, histograms of the *oD/pD* values computed for morphotype A and *E. subpertusa* specimens clearly show a bimodal distribution (Fig. 9), revealed also in the histograms of sample 161.01 mcd and of the samples above (Fig. 10). The specimens of the *Ericsonia subpertusa* have a maximum diameter size ≥ 5.5 and < 9 μm, and *oD/pD* values ≥ 0.3 and ≤ 0.45, corresponding to a Romein's ratio "central opening diameter/ring width" equal to 1-1.5. The specimens of the *Ericsonia robusta* morphotype A have a maximum diameter larger than *E. subpertusa,* ranging from 6 to 11 μm, and *oD/pD* values > 0.45 and ≤ 0.7 (Romein's ratio equal to 2-4), with most of the measured specimens having value 0.6. Morphologic differences between *Ericsonia robusta* morphotype A and *E. subpertusa* (Fig. 5; Pl. 1) result when specimens are observed in cross-polarized light, suggesting a different structure of the placolith. This is confirmed through S.E.M. observation: *Ericsonia subpertusa* specimens show the typical structure in the distal view of the wall with plate-like elements

imbricating clockwise (Pl. 2, figs 1, 2, 4). The distinction from *E. subpertusa* becomes more and more evident concomitantly with the emergence of the *E. robusta* morphotype B within the cluster of *E. robusta*, around 158 mcd in the section (Fig. 7a).

Both *Ericsonia robusta* morphotypes gradually increase in size throughout the studied interval (Fig. 7b). Morphotype B reaches a maximum diameter of 14-15 μm in the uppermost part of its range (Fig. 7b) but this increase in maximum size does not result in a proportional increase of the central opening, as indicated by *oD/pD* values that ranges from 0.4 to 0.6, with most of the measured specimens having value 0.5.

The distinction of the two morphotypes A and B of *Ericsonia robusta*, that is evident in the extinction patterns observed at cross-polarized light (Fig. 5, Plate 1), is not clearly revealed by morphometry. Throughout the studied interval, a unimodal distribution prevails in the histograms applied to the *oD/pD* parameter measured in the specimens counted in each sample (Fig. 11). The different extinction patterns are explained using the gypsum plate inserted in the light-beam, following Romein 1979's method described above. We could distinguish which side, proximal or distal, in each observed placolith was lying upward, and realized that morphotypes look different because some specimens had the distal side facing upwards whereas others had the proximal one (Fig. 4). It resulted that most of the observed *Ericsonia robusta* morphotypes A are views of proximal side (Pl. 1, figs 9-10; 23-25; Pl. 3, figs E-F; Pl. 4, figs 4,5), and the observed brighter inner cycle is the proximal shield. On the other hand, S.E.M. observation shows that *Ericsonia robusta* morphotype A and morphotype B have the same structures of the distal side (Pl. 3, figs 1-4; Pl. 4, figs 2, 3, 5, 6; Pl. 5, figs 1, 2, 4-6; Pl. 6, 1-6), with the wall elements covering the distal shield, notwithstanding that they have distinctively different relative size of the central opening. Moreover, the cover of calcite elements on the distal shield is thicker in morphotype B resulting in a brighter extinction pattern at cross-polarized light.

## Discussion

The analysis of the whole morphometric measurements obtained on the specimens of *Ericsonia robusta* group shows a limited degree of differentiation between the morphotypes A and B (Fig. 9), although the mean *oD/pD* value of morphotype A is generally higher than that of morphotype B (Figures 7a-b, 8). The structure of the two morphotypes is similar, as revealed by S.E.M. observations and corroborated by the unimodal distribution of the measured parameter *oD/pD* showed in the histograms of Fig. 11. Therefore, the two morphotypes document an intra-specific instead of an inter-specific variability. This variability extends from smaller placoliths (generally ≤ 10 μm) that have a relatively large central opening (mean *oD/pD* value ≥ 0.55 and ≤ 0.6), to larger placoliths (generally ≥

Plate 1

Polarizing microscope photomicrographs of Paleocene *Ericsonia* species and morphotypes. All specimens x 1200. Size bar = 5μm. PL = Parallel light; X-n = crossed nicols; gp = gypsum plate inserted.

1-3) *Ericsonia subpertusa*, distal side; 1. PL, 2. X-n, 3. gp. Sample 1262A-15H-4,17.
4-5) *E. subpertusa,* proximal side; 4. X-n, 5. gp. Sample 1262A-15H-4,17.
6-7) *E. robusta* morphotype A, proximal side; 6. PL, 7. X-n. Sample 1262A-15H-5,13.
8-10) *E. robusta* morphotype A, proximal side; 8. PL, 9. X-n, 10. gp. Sample 1262A-15H-4, 137.
11-13) *E. robusta* intermediate morphotype A - B, distal side; 11. PL, 12. X-n, 13. GP. Sample 1262A-15H-4,41.
14-15) *E. robusta* intermediate morphotype A - B, proximal side; 14. X-n, 15. gp. Sample 1262A-15H-4,41.
16-18) *E. robusta* intermediate morphotype A - B, distal side; 16. PL, 17. X-n, 18. gp. Sample 1262A-15H-4,17.
19-20) *E. robusta* intermediate morphotype A - B, proximal side; 19. X-n, 20. gp. Sample 1262A-15H-4,17.
21-22) *E. robusta* morphotype B, distal side; 21. X-n, 22. GP. Sample 1262A-15H-3,125.
23-25) *E. robusta* morphotype A, proximal side; 23. PL, 24. X-n, 25. GP. Sample 1262A-15H-2, 91.
26-27) *E. robusta* morphotype B, proximal side; 26. X-n, 27. gp. Sample 1262A-15H-2, 91.
28) *E. robusta* morphotype B, distal side; X-n. Sample 1262A-15H-2, 67.
29) *E. robusta* morphotype B, proximal side; X-n. Sample 1262A-15H-2, 67.
30) *E. robusta* morphotype B, proximal side; X-n. Sample 1262B-16H-6, 83.
31-32) *E. robusta* morphotype B, distal side; 31. X-n, 32. gp. Sample 1262B-16H-6, 53.
33-35) *E. robusta* morphotype A, proximal side; 33. PL, 34. X-n, 35. gp. Sample 1262B-16H-5, 119.
36) *E. robusta* morphotype B, distal side; X-n. Sample 1262B-16H-5, 95.
37) *E. robusta* morphotype B, proximal side; X-n. Sample 1262B-16H-5, 95.
38) *E. robusta* morphotype B, distal side; X-n. Sample 1262B-16H-5, 71.
39-40) *E. robusta* morphotype A, proximal side; 38. PL, 39. X-n, 40. gp. Sample 1262B-16H-5, 71.

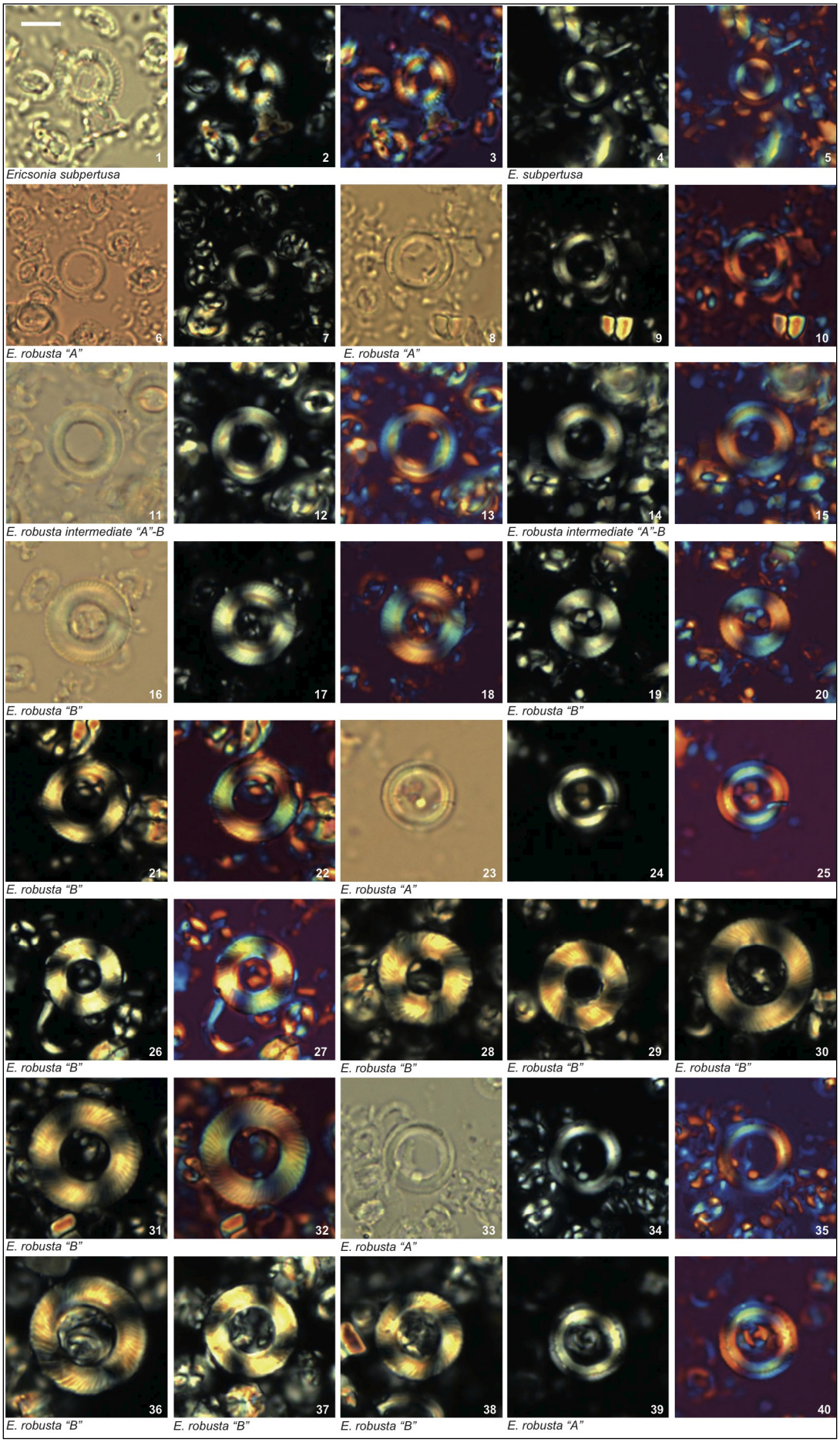
1
2
3
4
5
Ericsonia subpertusa
E. subpertusa
6
7
8
9
10
E. robusta "A"
E. robusta "A"
11
12
13
14
15
E. robusta intermediate "A"-B
E. robusta intermediate "A"-B
16
17
18
19
20
E. robusta "B"
E. robusta "B"
21
22
23
24
25
E. robusta "B"
E. robusta "A"
26
27
28
29
30
E. robusta "B"
E. robusta "B"
E. robusta "B"
31
32
33
34
35
E. robusta "B"
E. robusta "A"
36
37
38
39
40
E. robusta "B"
E. robusta "B"
E. robusta "B"
E. robusta "A"

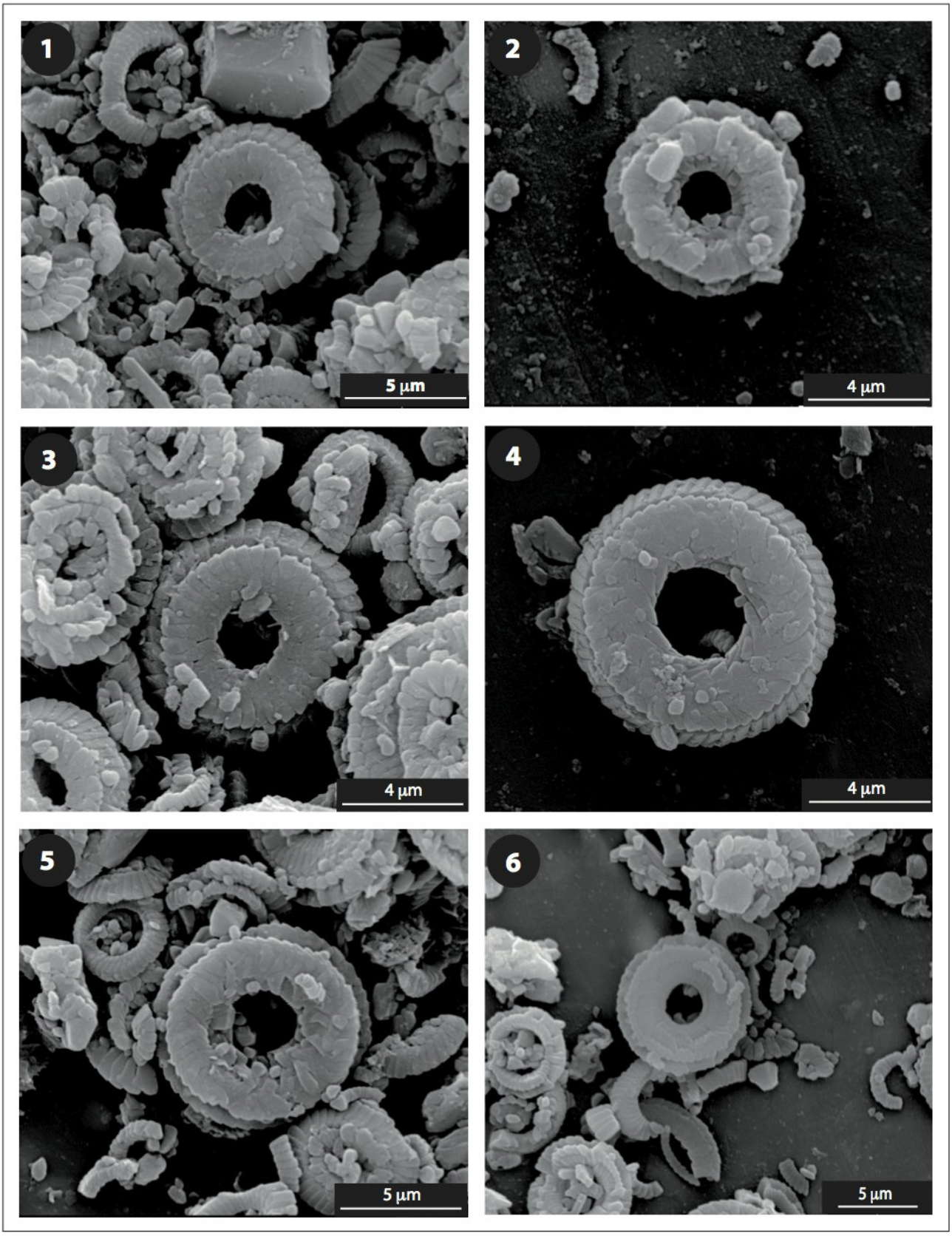


PLATE 2

S.E.M photomicrographs of *Ericsonia subpertusa*.
1) Sample 1262A-15H-4,17. Distal side. 2) Sample 1262A-15H-4,17. Proximal side. 3) Sample 1262A-15H-4,17. Distal side. 4) Sample 1262A-15H-4,17. Distal side. 5) Sample 1262A-15H-4,17. Proximal side. 6) Sample 1262A-15H-3,29. Proximal side.

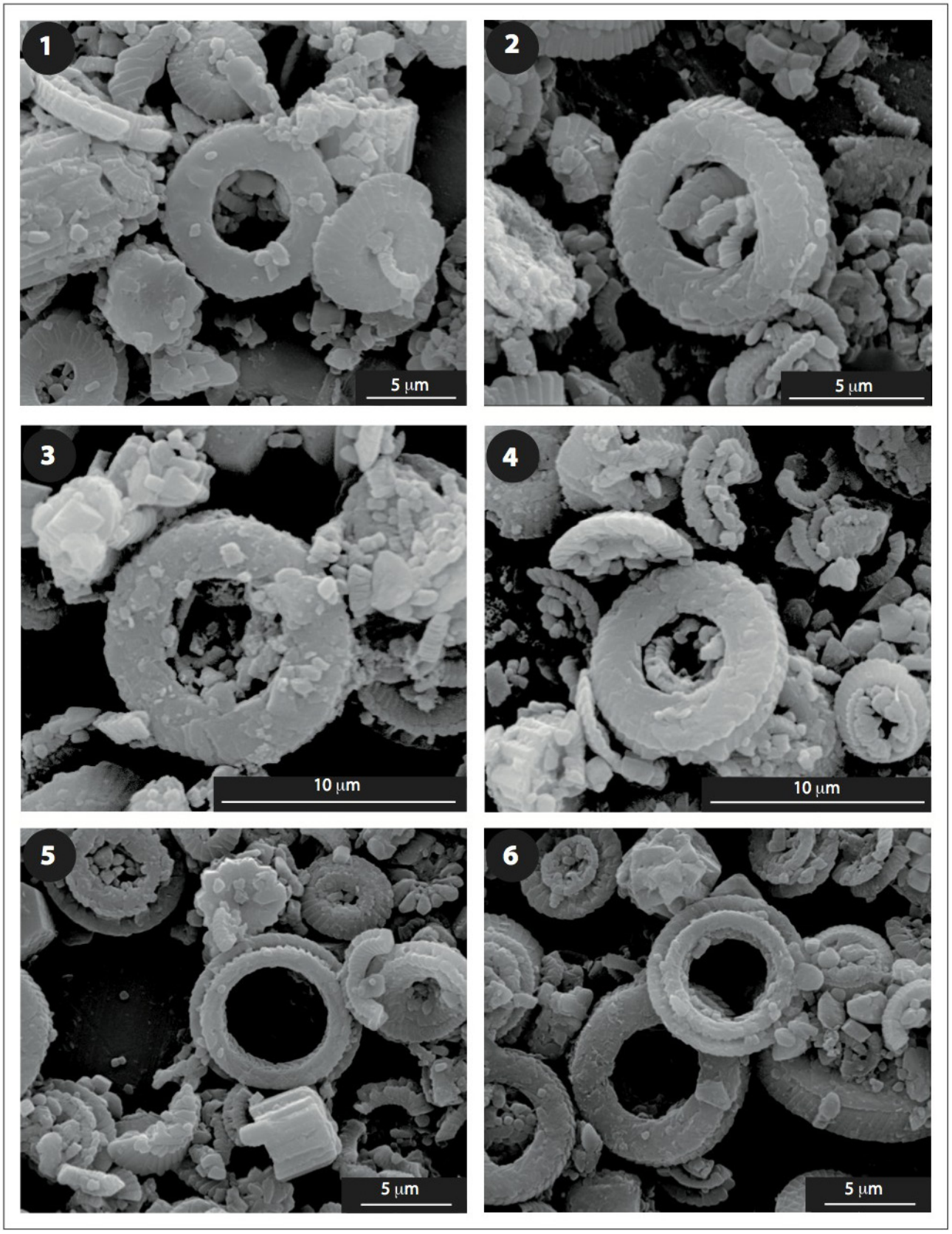


PLATE 3

S.E.M photomicrographs of *Ericsonia robusta* morphotype A specimens from the lower part of the studied ODP 1262 section.
1) Sample 1262A-15H-4,17. Distal side. 2) Sample 1262A-15H-4,17. Distal side. 3) Sample 1262A-15H-4,17. Distal side. 4) Sample 1262A-15H-4,17. Distal side. 5) Sample 1262A-15H-3,89. Proximal side. 6) Sample 1262A-15H-3,89. Proximal side.

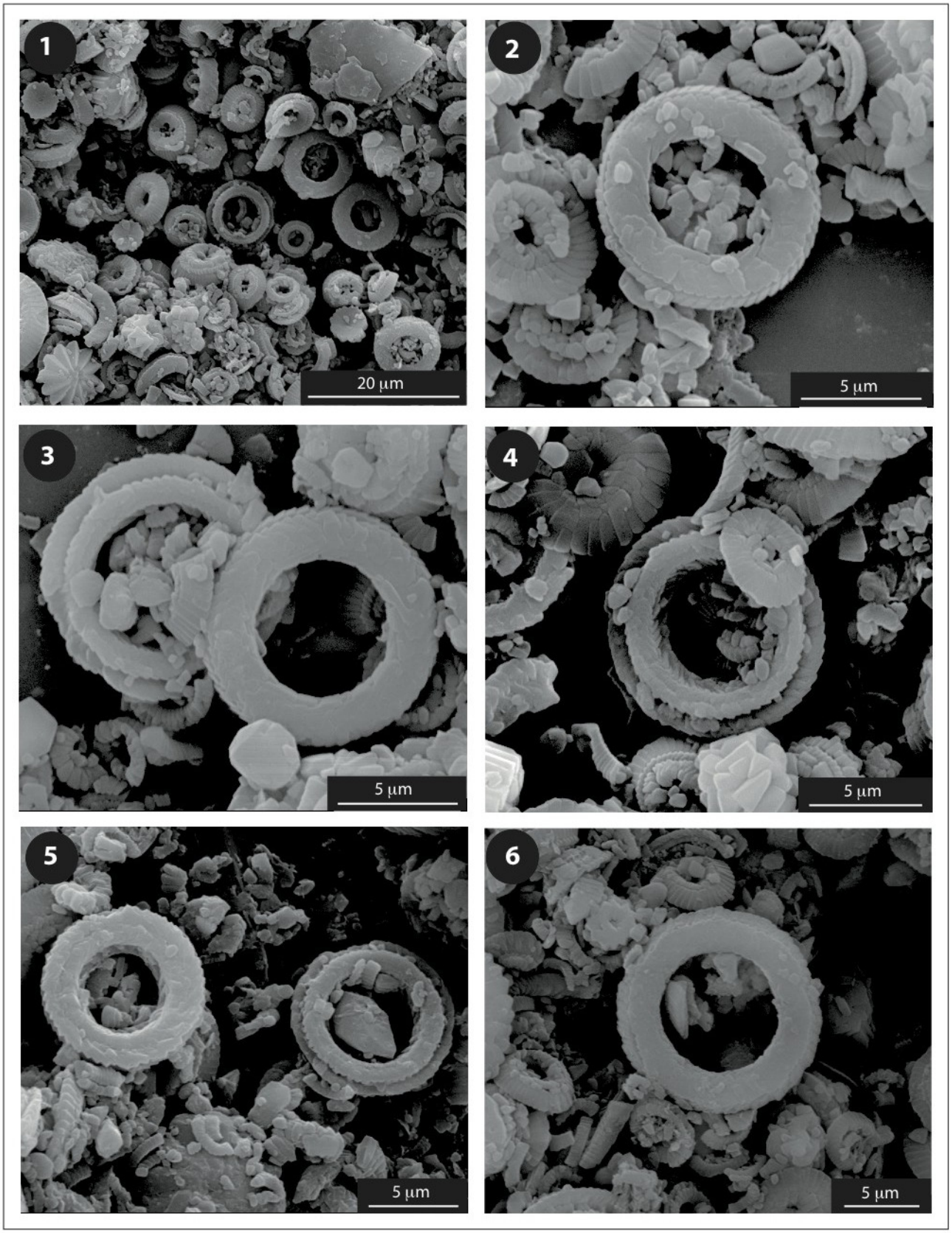


PLATE 4

S.E.M photomicrographs of *E. robusta* morphotype A specimens from the middle part of studied ODP 1262 section.
1) Sample 1262A-15H-3,29. 2) Sample 1262A-15H-3,29. Distal side. 3) Sample 1262A-15H-3,29. Proximal and distal sides. 4) Sample 1262A-15H-3,29. Proximal side. 5) Sample 1262A-15H-3,29. Distal and proximal sides. 6) Sample 1262B-16H-6,29. Distal side.

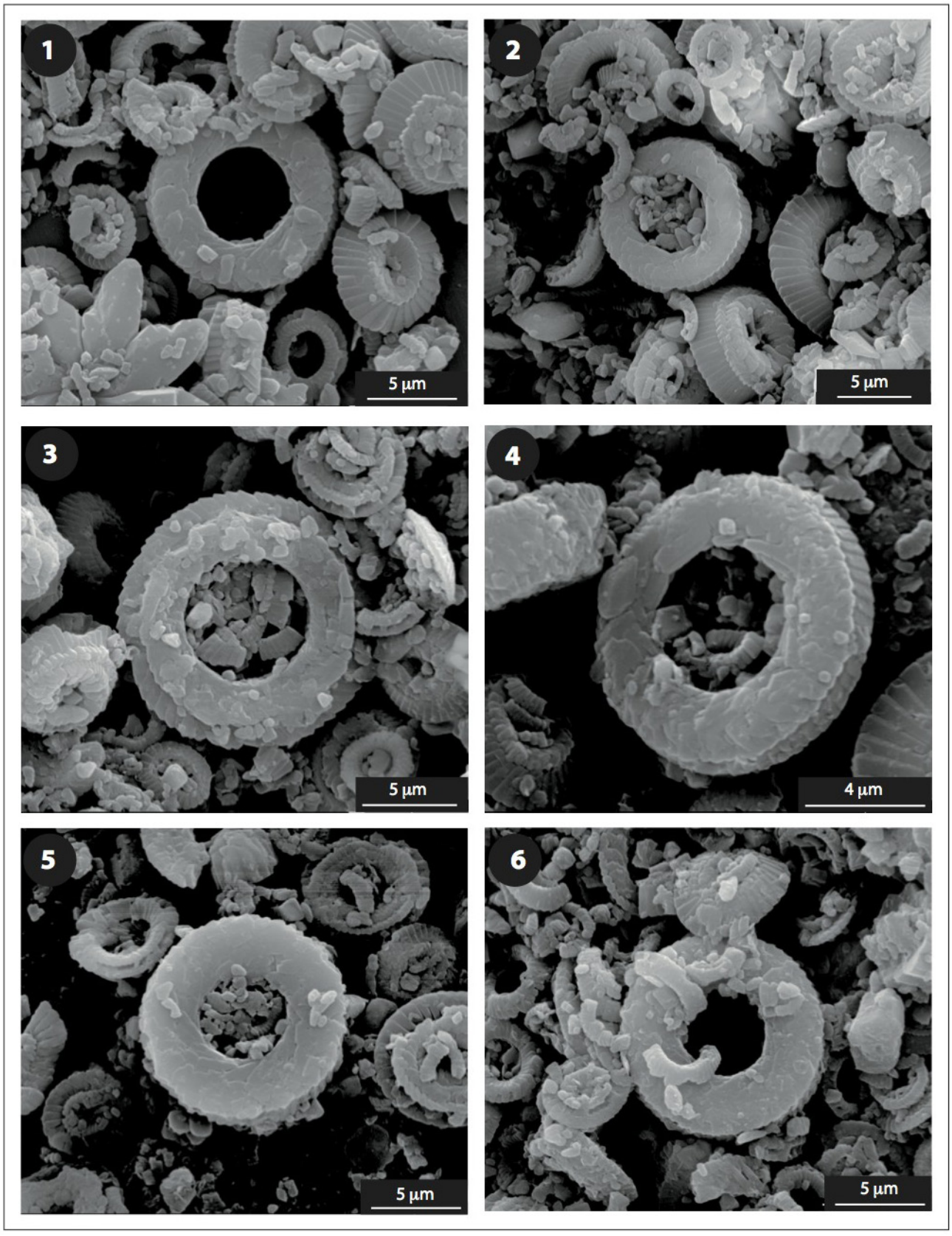


PLATE 5

S.E.M photomicrographs of *E. robusta* morphotype B from the studied ODP 1262 section.
1) Sample 1262A-15H-3,29. Distal side. 2) Sample 1262A-15H-3,29. Distal side. 3) Sample 1262A-15H-2,91. Proximal side. 4) Sample 1262A-15H-2,91. Distal side. 5) Sample 1262A-15H-2,91. Distal side. 6) Sample 1262A-15H-2,91. Distal side.

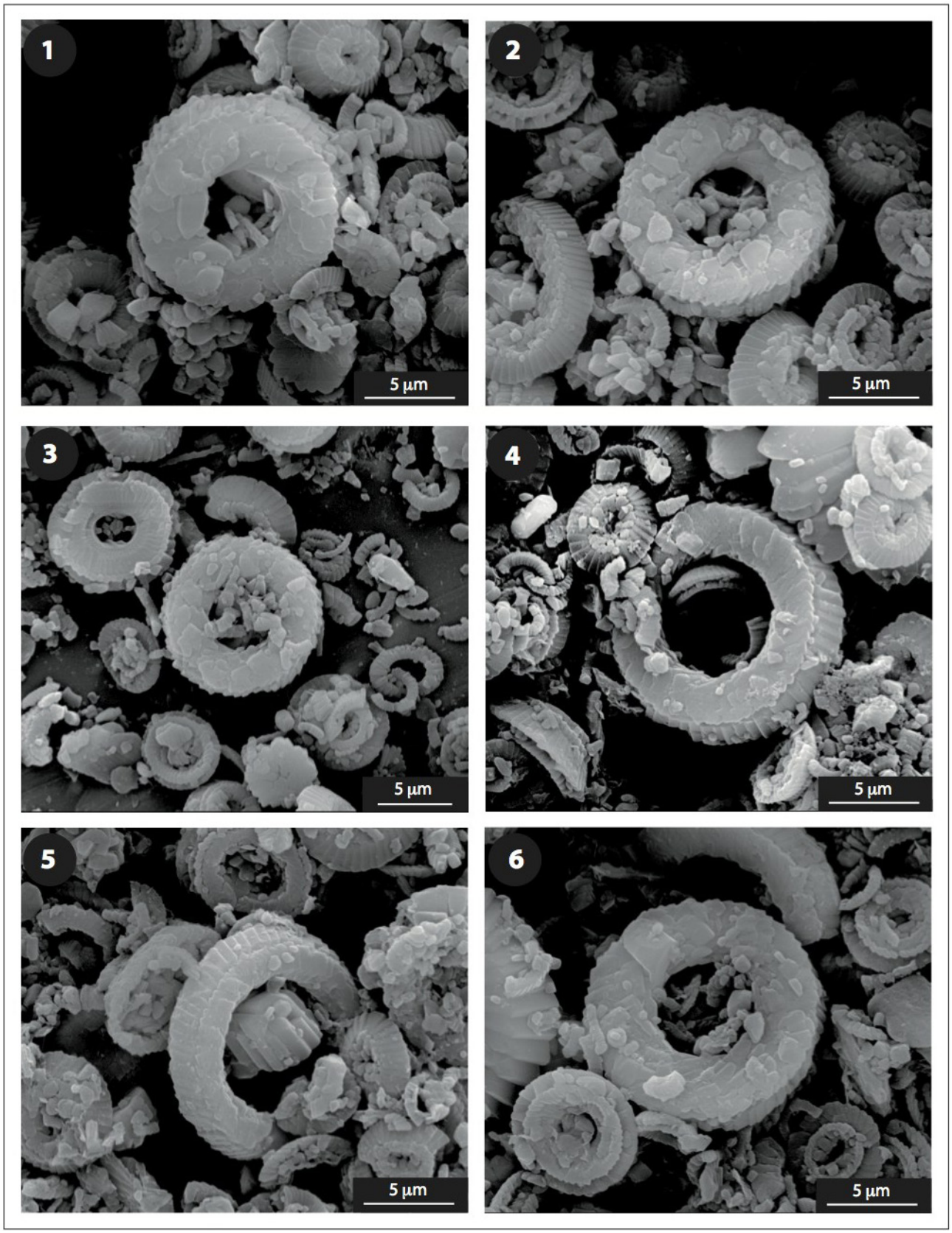


PLATE 6

S.E.M photomicrographs of *E. robusta* morphotype A and morphotype B specimens from the upper part of the studied ODP 1262 section.
1) Sample 1262B-16H-6,29. *Ericsonia robusta* morphotype B, distal side. 2) Sample 1262B-16H-6,29. *Ericsonia robusta* morphotype B, distal side. 3) Sample 1262B-16H-6,29. *Ericsonia robusta* morphotype B, distal side. 4) Sample 1262B-16H-5,119. *Ericsonia robusta* morphotype A, distal side. 5) Sample 1262B-16H-5,119. *Ericsonia robusta* morphotype A, distal side. 6) Sample 1262B-16H-5,119. *Ericsonia robusta* morphotype B, distal side.

11 μm) that do or do not have a proportionally large opening (mean *oD/pD* value ≥ 0.47 and ≤ 0.63) (Tab. 1). The specimens labelled morphotype B are distinguishable in cross-polarized light because they appear brighter (Pl. 1, figs 21-22; 26-32; 36-38) and prevail in the *Ericsonia robusta* pool in the upper part of its distribution range (Fig. 6). Based on these biometric data and conclusion, the species status for *Ericsonia universa* of Romein (1979), to which our *E. robusta* morphotype B could be referred for morphological similarity, is denied. Accordingly, we deny the species status for *E. aliquanta* (Bown, 2016) because it lacks distinctiveness of morphology in comparison with some specimens of *E. robusta*, and does not have a distinct stratigraphic range.

The data presented here add information about the evolutionary relationship among taxa included in the *Ericsonia* lineage reconstructed by Romein (1979). Differently from Romein's suggestion, we infer that *Ericsonia robusta* did not evolve from *E. subpertusa* on the basis of the following observations:

The lower range of *E. robusta* extends well below the level indicated by Romein (1979), because the first rare specimens, represented by *E. robusta* morphotype A, are observed in the lower part of the range of *Discoaster mohleri*, between 167 and 168 mcd (~58 Ma);

In the interval in which rare and scattered specimens of *E. robusta* morphotype A co-occur with *E. subpertusa* (from 168 to 158 mcd, corresponding to ~1 m.y.), specimens with intermediate morphology between the two species are not evident;

*E. subpertusa* and *E. robusta* morphotype A have placoliths with different central opening size (values of the ratio "*opening D/placolith D"* ranging from 0.3 to 0.4 in *E. subpertusa* and from 0.5 to 0.6 in *E. robusta* morphotype A), and a clearly different structure of the placolith as showed by S.E.M. observation. Specifically, the distal shield of *Ericsonia subpertusa* shows a steep outward slope in the margin, indicating a significantly elevated rim that has the elements of the inner wall that extend and cover part of it. These are plate-like elements strongly clockwise imbricating (Fig. 5; Pl. 2, fig. 1, 3). *Ericsonia robusta* morphotype A has a moderately elevated rim that in the distal side is completely covered by plate-like elements (Fig. 5; Pls 3-6).

As for the biostratigraphic results, it is noteworthy the distinct turnover in abundance between *Ericsonia robusta* and *E. subpertusa* observed at Site 1262 section within Chron C25n, preceding the lowest occurrence of *D. multiradiatus*. We did not record the same turnover in the nannofossil assemblages observed at Site 1215 that appear qualitatively and quantitatively different from those at Site 1262. The low sedimentation rate at Site 1215 section, and the corresponding sample spacing, did not permitted to obtain a more resolved biostratigraphy.

The biostratigraphic signal provided by the distribution range of *Ericsonia robusta* morphotype B is of some relevance and evidences an "ecological" link with *E. subpertusa*. *Ericsonia robusta* morphotype B increases in abundance concomitantly with the final decline of *E. subpertusa* followed by extinction, in the middle of Chron C25n. This turnover suggests a replacement in a portion of the same ecological niche. The subsequent final disappearance of morphotype B corresponds to the decline of the whole *E. robusta* group, and it is confirmed as a distinct biohorizon that occurs above the Base *D. multiradiatus* in both Site 1262 and 1215 sections. Note that a discrepancy exists in the position of Top *Ericsonia robusta* morphotype B relative to Top Chron C25n in the two studied sections: it occurs just below Top Chron C25n at ODP Site 1262 (between at 153.47 and 153.41 mcd) and just above Top Chron C25n at ODP Site 1215 (between 69.35 and 69.3 mcd), suggesting a diachrony of the biohorizon between the two different oceanic areas. *Ericsonia robusta* morphotype A is the only representative of *E. robusta* group after the decline and occurs with typical medium sized specimens (8-9 μm) that have a large central area and mean oD/pD value ≥ 0.6.

## Conclusions

Detailed biostratigraphic distribution of the genus *Ericsonia* in upper Paleocene deep-sea sediments from mid latitude Atlantic (ODP Site 1262) and tropical Pacific Ocean (ODP Site 1215) delineated the ranges of two taxonomic units within the genus, *E. subpertusa* and *E. robusta*. The obtained results help to clarify the taxonomic and evolutionary relationships within the Paleocene sector of *Ericsonia* lineage. *Ericsonia robusta* shows substantial morphologic variability (in the sizes of the placolith and the central opening) resulting in two endmember morphotypes: morphotype A with a larger cen-

tral opening, and morhotype B with a more robust structure. A notably different extinction pattern has been observed in many specimens of morphotype A when compared with morphotype B. In the early phase of the study, we thought that the two morphotypes could be indicative of two distinct species, morphotype A corresponding to the newly described *E. aliquanta*, and morhotype B to *E. robusta*. Instead, the differences observed are in part related to the different sides of the placoliths, that look different if some specimens have the distal side and others have the proximal side facing upwards in the field of view of the microscope. S.E.M. analyses revealed that the two morphotypes have a very similar structure of the placolith, even though they have different size of the central opening. The comparable placolith structure, together with the unimodal distribution of the parameter *oD/pD* measured in specimens through the section (Fig. 11), suggest that the two morphotypes represent intra-specific morpho-variants of the known species *Ericsonia robusta*. Specimens with intermediate morphologic features between the two end-member morphotypes are also observed throughout their distribution range.

*Ericsonia robusta* is rare and has a discontinuous distribution in the lower part of the studied interval at Site 1262, dominated by *E. subpertusa* that has its lowest occurrence in the lower Paleocene (Danian). The increases of *Ericsonia robusta* occurs in the upper Paleocene and characterizes the nannofossil assemblages during a 600 ky-time interval straddling Chron C25n (between ~57.2 and ~56.6 Ma). *Ericsonia subpertusa* and *E. robusta* co-occur in an interval of approximately 400 ky, but no evolutionary link between the two species has been documented. *Ericsonia subpertusa* declines (at ~56.9 Ma) towards extinction (at ~56.8 Ma) in the middle of Chron 25n, whereas *E. robusta* declines at ~56.6 Ma, when morphotype B became extinct.

The distinct turnover in abundance between *Ericsonia subpertusa* and *E. robusta*, that occurs within the lower part of Chron C25n and precedes the lowest occurrence of *D. multiradiatus*, and the disappearance of *E. robusta* morphotype B, are two noteworthy changes in the nannofossil assemblages in the late Paleocene. Preliminary data acquired on other nannofossil taxa (*Discoaster* and *Fasciculithus*), from the same C25n interval at Site 1262, show similar concurrent turnovers among species, and suggest that a further detailed analysis on nannofossil assemblages is required to reveal a possible coupling of the events and investigate on a possible common triggering.

*Acknowledgments*. Special thanks go to Letizia Di Bella for making available to us the S.E.M. at Dipartimento di Scienze della Terra, Università "La Sapienza" di Roma, and overall to Marco Albano for technical assistance with the S.E.M. and for plates composition. We used samples provided by the Ocean Drilling Program, sponsored by the US National Science Foundation and participating countries under the management of the Joint Oceanographic Institutions. We thank two anonymous reviewers for constructive comments and suggestions that helped to improve the manuscript. This research benefitted from the financial support to I.R. from the Università degli Studi "G. d'Annunzio" di Chieti-Pescara (Fondi Ateneo 2015-2016).

## References

Agnini C., Fornaciari E., Raffi I., Rio D., Röhl U., Westerhold, T. (2007) - High-resolution nannofossil biochronology of middle Paleocene to early Eocene at ODP Site 1262: Implications for calcareous nannoplankton evolution. *Mar. Micropaleontol.,* 64: 215-248. doi:10.1016/j. marmicro.2007.05.003.

Agnini C., Fornaciari E., Raffi I., Catanzariti R., Pälike H., Backman J., Rio D. (2014) - Biozonation and biochronology of Paleogene calcareous nannofossils from low and middle latitudes. *Newsl. Stratigr.*, 47(2): 131-181.

Arney J.E. & Wise S.W. Jr. (2003) - Paleocene–Eocene nannofossil biostratigraphy of ODP Leg 183, Kerguelen Plateau. In Frey, F.A., Coffin, M.F., Wallace, P.J., and Quilty, P.G. (Eds.), *Proc. ODP, Sci. Results*, 183: 1-59.

Black M. (1964) - Cretaceous and Tertiary coccoliths from Atlantic sea-mounts. *Paleontology,* 5: 306-316.

Backman J. (1986) - Late Paleocene to middle Eocene calcareous nannofossil biochronology from the Shatsky Rise, Walvis Ridge and Italy. *Palaeogeogr., Palaeoclimatol., Palaeoecol.,* 57: 43-59.

Bowles J. (2006) - Data report: revised magnetostratigraphy and magnetic mineralogy of sediments from Walvis Ridge, Leg 208. In: Kroon D., Zachos J.C. & Richter C. (Eds) - *Proc. ODP, Sci. Results,* 208: College Station, TX (Ocean Drilling Program): 1-24. doi:10.2973/odp.proc.sr.208.206.2006.

Bown P.R. & Young J.R. (1998) - Techniques. In: Bown P.R. (Ed.) - Calcareous nannofossil biostratigraphy. British Micropalaeontological Society Publication Series: 16-28. Chapman & Hall.

Bown P.R., Dunkley-Jones T., Lees J.A., Randell R.D., Mizzi J.A., Pearson P.N., Coxall H.K., Young J.R., Nicholas C.J., Karega A., Singano J. & Wade B.S. (2008) - A Paleogene calcareous microfossil Konservat-Lagerstätte from the Kilwa Group of coastal Tanzania. *GSA Bulletin,* 120: 3-12.

Bown P.R. (2016) - Paleocene calcareous nannofossils from Tanzania (TDP sites 19, 27 and 38). *J. Nannoplankton*

*Res.*, 36(1): 1-32.

Bralower T.J. & Mutterlose J. (1995) - Calcareous nannofossil biostratigraphy of ODP Site 865, Allison Guyot, Central Pacific Ocean: a tropical Paleogene reference section. *Proc. Ocean Drill. Program Sci. Res.,* 143: 31-72.

Bramlette M.N. & Sullivan F.R. (1961) - Coccolithophorids and related nannoplankton of the Early Tertiary in California. *Micropaleontol.,* 7: 129-188.

Hammer Ø., Harper D.A.T. & Ryan P.D. (2001) - PAST: Paleontological statistics software package for education and data analysis. *Palaeontol. Electr.* 4(1), 9 pp.

Hay W.W. & Mohler H.P. (1967) - Calcareous nannoplankton from early Tertiary rocks at Pont Labau, France, and Paleocene–early Eocene correlations. *J. Paleontol.*, 41(6): 1505-1541.

Littler K., Röhl U., Westerhold T. & Zachos J.C. (2014) - A high-resolution benthic stable-isotope record for the South Atlantic: Implications for orbital-scale changes in Late Paleocene–Early Eocene climate and carbon cycling. *Earth Plan. Sci. Letters,* 401: 18-30.

Lyle M. et al. (2002) - Proceedings of the Ocean Drilling Program. *Proc. Ocean Drill. Program, initial Rep.,* [CD-ROM], 199.

Martini E. (1971) - Standard Tertiary and Quaternary calcareous nannoplankton zonation. In: Farinacci A. (Ed.) - Proc. II Planktonic Conf, Roma, 1970, 2: 738-785. Roma (Tecnoscienza).

Okada H. & Thierstein H.R. (1979) - Calcareous plankton. Leg 43, *D.S.D.P., Initial Rep.,* 43: 507-573.

Perch-Nielsen K. (1977) - Albian to Pleistocene calcareous nannofossils from the Western South Atlantic, D.S.D.P. Leg 39. In: Supko P. R., Perch-Nielsen K. et al. - *D.S.D.P., Initial Rep.*, Washington, 39: 699-823.

Perch-Nielsen K. (1985) - Cenozoic calcareous nannofossils. In: Bolli H.M. et al. (Eds) - Plankton Stratigraphy: 427-554. Cambridge University Press, New York..

Raffi I., Backman J. & Pälike H. (2005) - Changes in calcareous nannofossil assemblage across the Paleocene/Eocene transition from the paleo-equatorial Pacific Ocean. *Palaeogeogr., Palaeoclimatol., Palaeoecol.*, 226: 93-126.

Romein A.J.T. (1979) - Lineages in early Paleogene calcareous nannoplankton. *Utrecht Micropaleont. Bull.* 22, 231 pp.

Westerhold T., Röhl U., Raffi I., Fornaciari E., Monechi S., Reale V., Bowles J. & Evans H. F. (2008) - Astronomical calibration of the Paleocene time. *Palaeogeogr., Palaeoclimatol., Palaeoecol.,* 257: 377-403.

Wise S.W., Wind F.H. (1977) - Mesozoic and Cenozoic calcareous nannofossils recovered by DSDP Leg 36 drilling on the Falkland Plateau, south-west Atlantic sector of the Southern Ocean. *D.S.D.P., Initial Rep.,* 36: 269-491.

Zachos J.C., Kroon D., Blum P. et al. (2004) - Early Cenozoic Extreme Climates: The Walvis Ridge Transect. *Proc. Ocean Drill. Program, Initial Rep.,* 208.

Zachos J.C., McCarren H., Murphy B., Röhl U. & Westerhold T. (2010) - Tempo and scale of late Paleocene and early Eocene carbon isotope cycles: implications for the origin of hyperthermals. *Earth Planet. Sci. Lett.* 299, 242-249.